Extended Abstracts of the 2001 International Conference on Solid State Devices and Materials, Tokyo, 2001, pp. 132–133

E-2-6

Magnetic and Optical Properties of (Ga,Mn)N

T. Kondo*, H. Owa, S. Kuwabara, and H. Munekata

Imaging Science and Engineering Laboratory, Tokyo Institute of Technology,
4259 Nagatsuda, Midori-ku, Yokohama 226-8503, Japan
**Contact Author; Phone/Fax:+81-45-924-5179, E-mail: tkondo@isl.titech.ac.jp*

1. Introduction

Studies on III-V-based magnetic alloy semiconductors (III-V-MAS) (or diluted magnetic semiconductors (III-V-DMS)) and carrier-induced magnetism have become one of the important research subjects for both semiconductors and magnetic materials. Up to now, narrow- and mid-gap III-V-MAS's have been realized with Mn[1-3] and Fe[4]. Efforts to prepare the wide-gap III-V-MAS based on GaN have been scarce. In this paper, we report on the magnetic and optical properties of *hexagonal* (Ga,Mn)N epilayers with the concentration of Mn ions being 10^{20} - 10^{21} cm^{-3}.

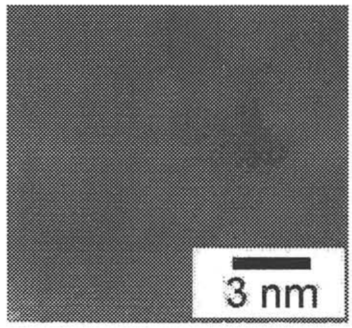

Fig. 2 High-resolution cross sectional TEM image for the (Ga,Mn)N sample No.257.

2. Sample Preparation

Samples were prepared by molecular beam epitaxy with an RF-plasma nitrogen source and elemental sources of Ga and Mn. In this study, T_s was varied between 500 and 800°C. A 10-nm thick GaN buffer layer was first deposited on the surface of a 2-μm thick hexagonal GaN epilayer grown by metal-organic vapor phase epitaxy on a sapphire (0001) substrate. This was followed by the epitaxy of 0.1-0.5 μm thick MAS layers. The deposition rate ranged from 30 to 150 nm/hr. When epitaxy is successful, the *in-situ* reflection high-energy electron diffraction pattern shows six-fold symmetric, streaky, (1×1) or (2×2) reconstructed pattern throughout the entire epitaxial process. The observed pattern indicates a Ga-terminated hexagonal surface. The HR-TEM image of (Ga,Mn)N only consists of the homogeneous lattice image due to the wurtzite structure. It should be also noted that the extended x-ray absorption fine structure analysis for (Ga,Mn)N samples indicates that Mn atoms are incorporated substitutionally in the Ga sub-lattice sites.

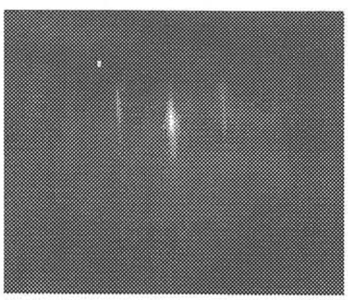

Fig. 1 A RHEED pattern observed along [11$\bar{2}$0] azimuth during the growth of a (Ga,Mn)N epilayer deposited at T_s = 600°C.

□□□ □□□□□□ □□□ □ □□□□□□□

Undoped-GaN epilayers exhibit *n*-type conduction with an electron concentration of n = 1-2 × 10^{18} cm^{-3} at room temperature. Photoluminescence spectrum of the (Ga,Mn)N sample with relatively low Mn concentration (~ $10^{18}cm^{-3}$) (Fig 3(b)) has noticeable peaks, except the peak originated from excitonic states, suggesting existence of Mn-acceptor level. As to the Mn-doped samples, the n value decreases monotonically with increasing Mn concentration up to mid 10^{18} cm^{-3}, and the samples become insulating by further Mn doping. They do not exhibit *p*-type conduction at present. In Fig. 4, we show the magnetization data obtained for the (Ga,Mn)N sample (No. 257). Paramagnetic behavior is predominant in the (Ga,Mn)N. However, there exists an *offset* component of about 6 emu/cm^3. We do not consider at present that this offset is due to the carrier-induced ferromagnetic order that was predicted for (Ga,Mn)N,[5] since the sample is highly resistive. Rather, it would be reasonable to assume the presence of the second phase. The Mn concentration contributing to the paramagnetism is estimated to be $[Mn]_{pm} = 8 \times 10^{20}$ cm^{-3} ($Ga_{0.98}Mn_{0.02}N$). From the Curie-Weiss plot, we obtain the paramagnetic Curie temperature $\theta_p \approx 20$ K and the effective spin number $S \approx 2.5$. The extracted S value suggests that the

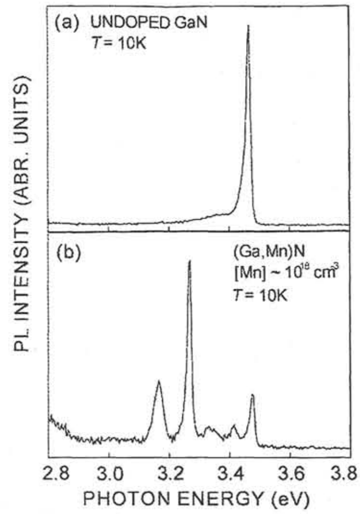

Fig.3 Photoluminescence spectra for (a) undoped-GaN epilayer and (b) (Ga,Mn)N epilayer with $[Mn]\sim10^{18}$ cm^{-3}.

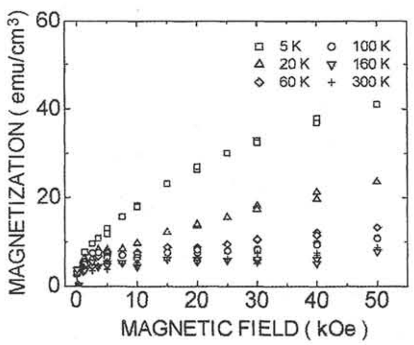

Fig.4 Magnetization data at various temperatures (5-300K) for the (Ga,Mn)N sample No.257.

ionic state of Mn ions contributing to the paramagnetic component is Mn^{2+} ($3d^5$). The positive θ_p value indicates Mn-Mn spin exchange interaction being slightly ferromagnetic.

In contrast to the high $[Mn]_{pm}$ samples, the paramagnetic Curie temperatures are negative in the samples with the low $[Mn]_{pm}$ values (~ 10^{19} cm^{-3}). Combining both low and high $[Mn]_{pm}$, we find that θ_p increases with $[Mn]_{pm}$. This fact indicates that the spin exchange interaction between Mn ions is antiferromagnetic in very diluted regime, but changes into ferromagnetic when $[Mn]_{pm}$ is increased. This trend is opposite to those observed for the paramagnetic II-VI and III-V DMS. In these cases, direct antiferromagnetic *d-d* spin exchange interaction increases with the Mn concentration. The origin of ferromagnetic spin exchange

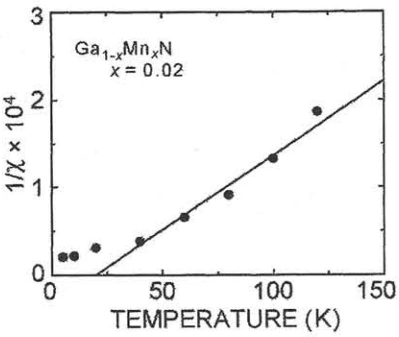

Fig. 5 Curie-Weiss plot for the (Ga,Mn)N sample (No.257) with $x = 0.02$.

in the (Ga,Mn)N may come from the exchange mechanism which is responsible for carrier-induced ferromagnetism.

□ □□□□□ □□□□□ □□□

Authors are grateful to A. Oiwa of Kanagawa Academy of Science and Technology (KAST) and S. Koshihara of Tokyo Institute of Technology and KAST for the collaboration in magnetization measurements. This work has been supported in part by the Ministry of ESSC Japan (grant No. 09244101), PRESTO of Japan Science and Technology Corporation, and NEDO International Joint Research Program.

□ □□□□□□□

[1] H. Munekata, H. Ohno, S. von Molnár, A. Segmüller, L. L. Chang, and L. Esaki: Phys. Rev. Lett. □□ (1989) 1849.

[2] H. Ohno, A. Shen, F. Matsukura, A. Oiwa, A. Endo, S. Katsumoto, and Y. Iye: Appl. Phys. Lett. □□ (1996) 363.

[3] T. Hayashi, M. Tanaka, T. Nishinaga, H. Shimada, H. Tsuchiya, and Y. Otuka: J. Cryst. Growth □□□□□□□ (1997) 1063.

[4] S. Haneda, M. Yamaura, Y. Takatani, K. Hara, S. Harigae, and H. Munekata: Jpn. J. Appl. Phys. □□ (2000) L9.

[5] T. Dietl, H. Ohno, F. Matsukura, J. Cibert, and D. Ferrand: Science □□□ (2000) 1019.